ELSEVIER

Thermochimica Acta 264 (1995) 41–58

thermochimica acta

# Thermodynamics of binary and ternary melts of the 3d transition metals (Cr, Mn, Fe, Co and Ni) with boron

V.T. Witusiewicz

*Institute for Foundry Problems, National Academy of Sciences of the Ukraine, 34/1 Vernadsky Ave., Kyyiv, 252680, Ukraine*

Received 21 June 1994; accepted 13 March 1995

**Abstract**

The thermodynamic functions (Gibbs energy, entropy) of mixing in the binary Fe–B, Co–B and Ni–B systems were determined using experimental activity data from the literature and the enthalpy data of the alloy formation measured earlier by the author. The excess entropies of mixing were found to be largely negative, indicating the existence of short-range ordering in these liquid alloys. A short description of the experimental method for a ternary system and an example of the original values measured in a separate experiment are given. The partial and integral enthalpies of formation of the ternary Cr–Fe–B, Mn–Fe–B, Co–Fe–B and Ni–Fe–B melts were measured directly using a high-temperature isoperibolic calorimeter. The large negative enthalpies of mixing in all the studied ternary systems reflect the strong interaction of the alloy components. The existence of attractive forces between unlike atoms of the 3d transition metals in the ternary alloys causes a decrease in the absolute values of the partial enthalpy of mixing of boron. Comparing the experimental data with the data interpolated from the binary boundary systems using well-known models, it was shown that these models in most cases are incorrect for the ternary Cr(Mn,Co,Ni)–Fe–B melts. Using the measured data, the glass-forming ability of the ternary melts is discussed.

*Keywords:* Excess entropy; Gibbs energy; Glass-forming ability; Isoperibolic calorimeter; Mixing enthalpy

## 1. Introduction

The melts of the 3d transition metals (Tr is Cr, Mn, Fe, Co or Ni) are widely used for the production of several kinds of high-magnetic-permeability metallic amorphous materials, using rapid quenching. The thermodynamic data for such liquid alloys are


*SSDI* 0040-6031(95)02345-3

important for the solution of practical high-temperature problems, particularly for the prediction of glass-forming ability in these alloys. In recent years, the activities of the components in the binary Fe–B, Co–B and Ni–B systems were measured by the electromotive forces method [1, 2] and the Knudsen effusion technique [3]. The partial and integral enthalpies of formation of the binary Tr–B alloys have been determined by calorimetry [4–10]. As a continuation of the previous investigations, excess thermodynamic functions of mixing in binary Fe–B, Co–B and Ni–B melts were calculated using the above-mentioned data and the alloy thermochemistries of the ternary Cr–Fe–B, Mn–Fe–B, Co–Fe–B and Ni–Fe–B systems were studied experimentally by isoperibolic calorimetry.

## 2. Calculations and experimental details

To determine the excess thermodynamic functions, the experimental activity data measured by Yukinobu et al. [1], and Ushio and Ogawa [2] were statistically treated by least squares analysis using the equation

$$\ln \gamma_2 = (1-x)^2 \alpha \tag{1}$$

where $\gamma_2$ and $x$ are the activity coefficient and molar fraction of boron, respectively. The $\alpha$ functions were represented as a simple empirical power series expansion versus the boron mole fraction. The activity coefficients of the 3d transition metals, $\gamma_1$ were determined by means of the Gibbs–Duhem equation using the $\alpha$ functions

$$\ln \gamma_1 = -\alpha(1-x)x + \int_0^x \alpha \mathrm{d}x \tag{2}$$

The activity data mentioned above and described by Storms and Szklarz [3] are given with the reference state being solid 3d metals and solid boron. Therefore, for the determination of the excess Gibbs energy of mixing and the characterization of the interaction of the components, these data were converted to the reference state of the liquid metal and liquid boron, using well-known equations [11]. Since the differences in heat capacities of the solid and liquid components are negligibly small, it was assumed that the enthalpies of mixing do not depend on temperature. Therefore, the basic equations are simplified as

$$\Delta_m \bar{G}_i^{ex} = \Delta_s \bar{G}_i^{ex} - \Delta_f H_i^0 \left(1 - \frac{T}{T_{f,i}}\right) \tag{3}$$

and

$$\Delta_m \bar{H}_i = \Delta_s \bar{H}_i - \Delta_f H_i^0 \tag{4}$$

where $\Delta \bar{G}_i^{ex}$ and $\Delta \bar{H}_i$ are the partial molar excess Gibbs energy and partial enthalpy of component $i$ referred to the solid (subscript s) or liquid (subscript m) pure component $i$; $\Delta_f H_i^0$ and $T_{f,i}$ are the enthalpy changes of fusion of one mole of component $i$ and the absolute temperature of fusion of this component respectively; and $T$ is the temperature of the activity measurement. Values adopted for $\Delta_f H_i^0$ and $T_{f,i}$ (50.2 kJ mol$^{-1}$, 2348 K) were taken from the literature [12, 13].

The enthalpies of formation of the ternary liquid Tr–Fe–B alloys were investigated using the high-temperature isoperibolic calorimeter, provided with a system of data accumulation and mathematical treatment by personal computer. The apparatus was applied as a drop calorimeter with constant temperature. The heat effects were measured by successive introductions of samples (3d metal or boron) at a standard temperature (298 K) into a liquid bath (binary or ternary alloy). Temperature measurements were carried out with a thermocouple (WRe5–WRe20, calibrated using pure substances as recommended by the International Temperature Scale of 1990) protected by a yttria-stabilized zirconia shield and placed in the melt. The temperatures at which the experiments were carried out were $2150 \pm 15$ K for the Cr–Fe–B system, $1830 \pm 10$ K for Mn–Fe–B, $1900 \pm 15$ K for Co–Fe–B and $1873 \pm 10$ K for Ni–Fe–B. The initial mass of alloy in the calorimetric crucible was 40–60 g. To obtain partial molar enthalpies of alloy formation, the dropping sample mass was controlled by a computer so that the concentration changes in the bath did not exceed 1%at. A stirrer ensured complete and rapid dissolution or mixing of the components. The material of the crucible and the stirrer was the same as the thermocouple shield. The experiments were carried out in purified helium at an excess pressure of $5 \times 10^3$ Pa. The purities of the metals and metalloids were (in %): 99.8 for Cr, 99.6 for Mn and Fe, 99.95 for Co and Ni, and 99.5 for crystalline B. The measurements were carried out on ray sections (the concentration ratio of the initial components in the alloys was kept constant for the total running time) with $x_{TR}:x_{Fe}$ being 0.25:0.75, 0.5:0.5, 0.75:0.25 and 0.9:0.1 (the latter only for Ni–Fe–B alloys).

The alloy formation enthalpies were calculated using the method described earlier in Refs. [14] and [15]. Note that the method takes into account some temperature drift during a measurement and does not require a permanent calibration of the calorimeter by a standard inert sample which represents an additional source of melt contamination. The thermal equivalent of the calorimeter, $W(x)$, is derived directly using the Gibbs–Duhem equation from the concentration dependences of the areas under the temperature–time curves (referred to 1 mol of a component $i$), $F_i(x)$, which are due to the solution of each component. This approach results in thermodynamically consistent data [14]. Thus, in the case of a ternary system if the concentration ratio of the components of an initial binary alloy remains constant within the run, the enthalpies of mixing may be determined using the expressions

$$\Delta\bar{H}_i(x) = -\Delta H^{T^\circ}_{298,i} - \Delta c_{p,i}\Delta T(x) + W(x)F_i(x) \quad i = 1,2,3 \tag{5}$$

$$\Delta H(x) = (1-x)(1-y)\Delta\bar{H}_1(x) + (1-x)y\Delta\bar{H}_2(x) + x\Delta\bar{H}_3(x) \tag{6}$$

$$\mathrm{d}W(x) = -\frac{1}{\Phi_\Sigma(x)}\left[W(x)\mathrm{d}\Phi_\Sigma(x) + W(x)\frac{\Phi_\Sigma(x) - F_3(x)}{1-x}\mathrm{d}x - \Delta C_{p,\Sigma}(x)\mathrm{d}T(x)\right] \tag{7}$$

$$\Phi_\Sigma(x) = (1-x)(1-y)F_1(x) + (1-x)yF_2(x) + xF_3(x) \tag{8}$$

$$\Delta C_\Sigma(x) = (1-x)(1-y)\Delta c_{p,1} + (1-x)y\Delta c_{p,2} + x\Delta c_{p,3} \tag{9}$$

where $\Delta H^{T^\circ}_{298,i}$, $\Delta c_{p,i}$, and $\Delta\bar{H}_i(x)$ are the standard enthalpies of heating, the heat capacity and the concentration dependence of the partial melt formation enthalpy

component $i$, respectively; $\Delta H(x)$ is the integral enthalpy of alloy formation of the ray section with constant ratios of $y/(1-y)$. The value $\Delta T(x) = T(x) - T^0$ is the difference between the temperature values at every drop, $T(x)$, and the initial value $T^0$, fixed at $x = 0$; $y$ and $x$ are the mole fractions of the second component (Cr, Mn, Co or Ni) in the initial binary alloy, and the third component (B) in the ternary melt.

The differential equation, Eq. (7), does not allow division by the variables; therefore the numerical method of solution was applied. The initial expression for $x = 0$ is

$$W(0) = \frac{(1-y)\Delta H^{T^o}_{298,1} + y\Delta H^{T^o}_{298,2} + \Delta H^0}{(1-y)F_1(0) + yF_2(0)} \tag{10}$$

where $\Delta H^0$ is the integral enthalpy of formation of the initial binary alloy. As one can see from Eq. (7), difficulties in the numerical integration may arise when $\Phi_\Sigma(x)$ is equal or near to zero. However, in all the studied Tr–Fe–B melts, this was not observed. The standard values of the enthalpies of heating of the components were taken from Refs. [12] and [13]. The integral enthalpies of mixing of the components at ultimate dilution in the systems Cr–Fe, Mn–Fe, Co–Fe and Ni–Fe, which are necessary for the calculation of $W(0)$, were adopted from Refs. [16–19], which are considered to be the most reliable, and are listed in Table 1. Table 2, as an example, presents the original values measured in a separate experiment (the composition of the starting sample; the amount of the sample dropped, $m_i$; the mole fraction of boron, $x_B$; the area under the temperature–time curve, $F_i$; the temperature of the liquid bath at each dropping, $T_i$) and the values of the partial enthalpies of mixing of liquid Cr, Fe and a solution of crystalline B, $\Delta\bar{H}_i$, calculated using Eqs. (5)–(10) for ternary alloys of the ray section $(Fe_{0.25}Cr_{0.75})_{1-x}B_x$. The initial mass of the binary alloy in the calorimeter was equal to 58.00 g and the temperature of the dropped samples was 298 K. Standard enthalpies of heating from 298 K to $T^0 = 2165$ K and the heat capacities of Cr, Fe and B at the temperature of the experiment according to Refs. [12] and [13] were taken as 95.90, 89.80, and 48.05 kJ mol$^{-1}$, and 50.00, 44.58, and 30.00 J mol$^{-1}$ K$^{-1}$, respectively. Finally, the integral enthalpy of formation of the initial binary alloy $Cr_{0.75}Fe_{0.25}$, $\Delta H^0$, was taken as $-3.0$ kJ mol$^{-1}$ [16].

Table 1
Integral enthalpies of mixing in boundary binary Tr–Fe systems

| Molar fraction of Tr metals | $-\Delta_m H^0$/kJ mol$^{-1}$ | | | |
|---|---|---|---|---|
| | Cr–Fe [16] | Mn–Fe [17] | Co–Fe [18] | Ni–Fe [18, 19] |
| 0 | 0 | 0 | 0 | 0 |
| 0.10 | 1.3 | 1.3 | 0.7 | 1.0 |
| 0.25 | 2.9 | 3.0 | 1.6 | 2.3 |
| 0.50 | 3.6 | 4.9 | 2.4 | 4.1 |
| 0.75 | 3.0 | 4.4 | 1.9 | 4.4 |
| 0.90 | 1.4 | 2.3 | 0.9 | 2.6 |
| 1.00 | 0 | 0 | 0 | 0 |

Table 2
The original experimental values (the amount of the sample dropped $m_i$; the boron mole fraction $x_B$; the temperature of the liquid bath at each dropping $T_i$; the area under the temperature–time curve $F_i$; and the partial enthalpies of mixing of liquid Cr, Fe and solution of crystalline B $\Delta\bar{H}_i$) for ternary alloys of the ray section $(Fe_{0.25}Cr_{0.75})_{1-x}B_x$

| Starting sample: 43.00 g Cr + 15.00 g Fe | | | | | | | | | | | |
|---|---|---|---|---|---|---|---|---|---|---|---|
| $i$ | $m_i$/g | $x_B$ | $F_i$/K s mol$^{-1}$ | $T_i$/K | $\Delta\bar{H}_i$/ kJ mol$^{-1}$ | $i$ | $m_i$/g | $x_B$ | $F_i$/K s mol$^{-1}$ | $T_i$/K | $\Delta\bar{H}_i$/ kJ mol$^{-1}$ |
| Cr | 0.441 | 0 | 444.5 | 2165 | 0.3 | Cr | 0.520 | 0.180 | 340.9 | 2149 | −12.2 |
| Fe | 0.261 | 0 | 365.2 | 2165 | −10.7 | Cr | 0.492 | 0.179 | 340.5 | 2149 | −12.1 |
| Cr | 0.440 | 0 | 435.8 | 2165 | −1.6 | Fe | 0.406 | 0.178 | 363.0 | 2148 | −0.9 |
| Fe | 0.262 | 0 | 366.4 | 2165 | −10.5 | B | 0.181 | 0.187 | −3.1 | 2148 | −48.8 |
| B | 0.080 | 0.007 | −114.3 | 2165 | −72.7 | B | 0.170 | 0.196 | −0.1 | 2147 | −48.1 |
| B | 0.101 | 0.015 | −118.2 | 2165 | −73.8 | B | 0.173 | 0.204 | −6.7 | 2147 | −49.8 |
| B | 0.097 | 0.022 | −144.4 | 2165 | −79.5 | B | 0.172 | 0.212 | 8.9 | 2146 | −45.7 |
| B | 0.080 | 0.029 | −124.8 | 2164 | −75.3 | B | 0.202 | 0.222 | 30.2 | 2146 | −40.0 |
| B | 0.102 | 0.037 | −119.7 | 2164 | −74.3 | B | 0.204 | 0.231 | −24.9 | 2145 | −41.3 |
| B | 0.103 | 0.044 | −115.6 | 2164 | −73.4 | Cr | 0.496 | 0.229 | 320.8 | 2145 | −9.1 |
| Cr | 0.432 | 0.044 | 435.0 | 2164 | −0.4 | Cr | 0.552 | 0.229 | 282.1 | 2144 | −19.9 |
| Fe | 0.252 | 0.044 | 354.3 | 2163 | −12.0 | Fe | 0.480 | 0.227 | 340.1 | 2144 | 1.6 |
| Cr | 0.440 | 0.044 | 440.8 | 2163 | 0.8 | B | 0.225 | 0.236 | 12.2 | 2143 | −44.7 |
| Fe | 0.256 | 0.044 | 371.5 | 2163 | −8.3 | B | 0.245 | 0.247 | 28.0 | 2143 | −40.1 |
| B | 0.102 | 0.051 | −111.7 | 2162 | −72.6 | B | 0.204 | 0.255 | 33.0 | 2142 | −38.5 |
| B | 0.101 | 0.058 | −121.1 | 2162 | −74.8 | B | 0.214 | 0.264 | 40.0 | 2142 | −36.2 |
| B | 0.100 | 0.065 | −113.0 | 2162 | −73.0 | B | 0.232 | 0.273 | 44.4 | 2142 | −34.6 |
| B | 0.106 | 0.073 | −120.8 | 2161 | −74.9 | B | 0.246 | 0.282 | 53.5 | 2141 | −31.4 |
| B | 0.107 | 0.080 | −123.8 | 2161 | −75.6 | Cr | 0.462 | 0.281 | 263.6 | 2141 | −14.2 |
| B | 0.111 | 0.088 | −127.5 | 2160 | −76.6 | Cr | 0.446 | 0.280 | 234.4 | 2141 | −23.5 |
| Cr | 0.432 | 0.087 | 423.7 | 2160 | −1.2 | Fe | 0.331 | 0.279 | 318.9 | 2140 | 8.4 |
| Cr | 0.433 | 0.086 | 410.2 | 2159 | −4.2 | B | 0.222 | 0.289 | 50.5 | 2140 | −32.1 |
| Fe | 0.331 | 0.086 | 366.5 | 2159 | −7.9 | B | 0.265 | 0.297 | 53.3 | 2140 | −30.8 |
| B | 0.117 | 0.094 | −139.9 | 2158 | −79.4 | B | 0.263 | 0.306 | 52.6 | 2140 | −30.5 |
| B | 0.111 | 0.101 | −123.4 | 2158 | −75.9 | B | 0.250 | 0.314 | 46.2 | 2139 | −32.3 |
| B | 0.130 | 0.109 | −115.7 | 2157 | −74.3 | B | 0.280 | 0.324 | 48.5 | 2139 | −31.1 |
| B | 0.138 | 0.118 | −93.9 | 2157 | −69.5 | B | 0.300 | 0.334 | 50.5 | 2139 | −30.1 |
| B | 0.129 | 0.125 | −129.6 | 2156 | −77.8 | Cr | 0.506 | 0.332 | 195.4 | 2139 | −26.6 |
| B | 0.131 | 0.133 | −69.6 | 2156 | −64.2 | Cr | 0.465 | 0.330 | 192.3 | 2139 | −27.9 |
| Cr | 0.498 | 0.132 | 403.5 | 2155 | −2.7 | Fe | 0.337 | 0.329 | 298.2 | 2139 | 15.4 |
| Cr | 0.500 | 0.131 | 394.6 | 2155 | −4.8 | B | 0.291 | 0.338 | 46.9 | 2139 | −31.2 |
| Fe | 0.340 | 0.131 | 374.1 | 2154 | −3.4 | B | 0.281 | 0.347 | 42.8 | 2139 | −32.5 |
| B | 0.155 | 0.140 | −38.5 | 2153 | −57.0 | B | 0.303 | 0.356 | 49.1 | 2139 | −30.0 |
| B | 0.161 | 0.149 | −62.3 | 2153 | −62.7 | B | 0.265 | 0,364 | 49.7 | 2139 | −29.7 |
| B | 0.155 | 0.158 | −54.6 | 2152 | −61.0 | B | 0.311 | 0.373 | 47.7 | 2139 | −30.5 |
| B | 0.154 | 0.166 | −26.8 | 2152 | −54.5 | B | 0.304 | 0.381 | 46.4 | 2139 | −31.1 |
| B | 0.152 | 0.174 | −2.9 | 2151 | −48.8 | Cr | 0.481 | 0.379 | 195.0 | 2139 | −24.5 |
| B | 0.165 | 0.183 | −5.4 | 2151 | −49.4 | Cr | 0.460 | 0.378 | 191.8 | 2140 | −25.5 |
| Cr | 0.404 | 0.182 | 350.6 | 2150 | −9.6 | Fe | 0.395 | 0.376 | 297.1 | 2140 | 19.4 |

## 3. Results and discussion

### 3.1. Thermodynamics of Tr–B melts

The enthalpies of formation of liquid Cr(Mn, Fe, Co, Ni)–B alloys have been experimentally determined previously [4–10]. The concentration dependences of partial functions in the Fe–B system ($T = 1900$ K) between 0.40 and 0.54 and above 0.60 boron mole fractions show evidently horizontal segments (Fig. 1 [4]). At the time of the experiment, the phase diagram of the Fe–B system published in Ref. [20] was considered, containing two intermetallic compounds, FeB and $FeB_2$, melting congruently at 1813 and 2343 K respectively. Therefore, the formation of associates of FeB in the first and of boride $FeB_2$ in the second concentration regions of the liquid alloys

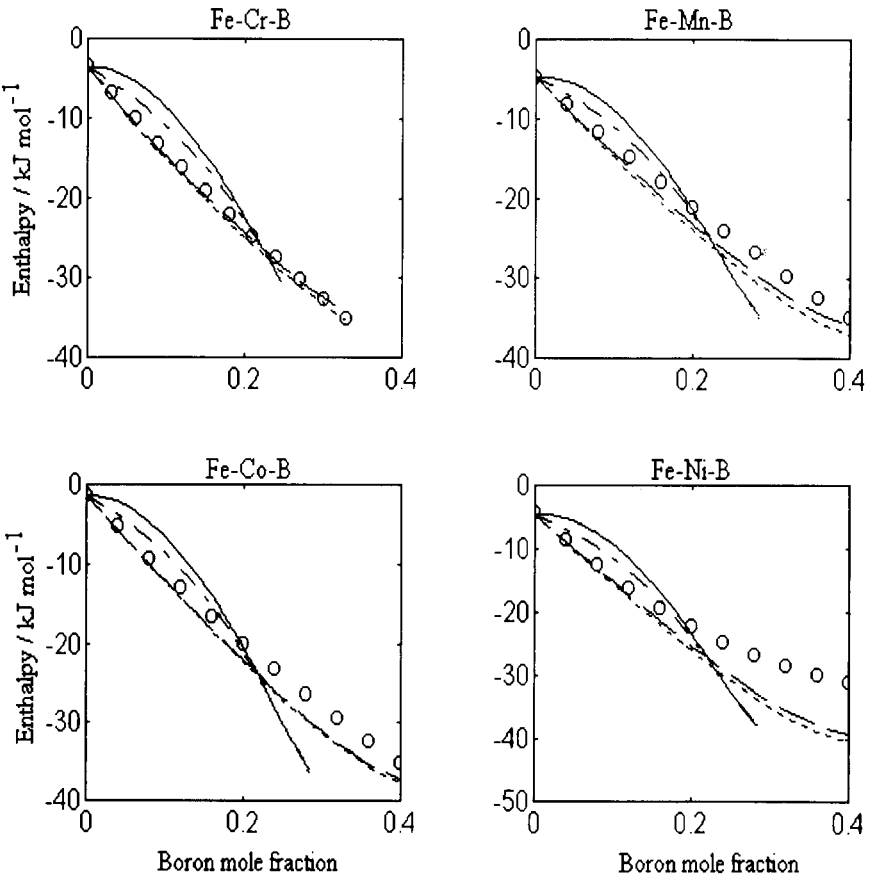


Fig. 1. Comparison of the experimental values (circles) of the integral enthalpy of mixing for the $(Fe_{0.5}Tr_{0.5})_{1-x}B_x$ melts with the values interpolated from binary boundary systems using Kohler's (dash-dotted lines), Toop's ( dashed lines ), Bonnier's ( dotted lines) and Muggianu's (solid lines) algorithms [24].

mentioned above was assumed. Later investigations of the phase diagram [21,22] showed that the FeB compound melts at 1923 K, about 20 K higher than the temperature of the enthalpy measurements in Ref. [4], and that the intermetallic compound $FeB_2$ is completely absent. So, the first horizontal segment corresponds to heterogenous phase fields (liq. + FeB) and the second is due to the approach towards the boron-saturation boundary. Moreover, the partial enthalpies of mixing in the Fe–B as well as in the Cr–B [9] systems also reveal some peculiarities (both have a horizontal segment) at a boron mole fraction of 0.25. The mentioned melts near this concentration of boron are in the proximity of the formation of $Fe_3B$ and $Cr_3B$ associates respectively. The concentration dependences of the partial enthalpies of the Mn–B, Co–B and Ni–B alloys [6–9] do not reveal any effects; up to $x = 0.2$, they may be described by a simple dilute solution model.

Combining the concentration dependences of the experimental enthalpies [4, 6–8] with the statistically treated activity data [1–3] (the latter values for Cr–B and Mn–B melts are absent in the literature), the excess partial and integral entropies for liquid Fe–B, Co–B and Ni–B alloys were calculated. Overall, the thermodynamic functions (partial enthalpies and partial excess mixing entropies of boron) from 0 to 0.50 mole fractions of boron may be represented by following equations (with $\Delta\bar{H}_B$ in kJ mol$^{-1}$, $\Delta\bar{S}_B^{ex}$ in J mol$^{-1}$ K$^{-1}$, and $x = x_B$.

For the Cr–B system

$$\Delta\bar{H}_B = (1-x)^2(-141.6 - 487.4x + 3840.1x^2 + 53510.8x^3 - 831211.7x^4 + 3467524.5x^5 - 4604435.6x^6)$$

For the Mn–B system

$$\Delta\bar{H}_B = (1-x)^2(-111.6 - 184.9x - 140.3x^2 - 433.9x^3 + 4435.4x^4)$$

For the Fe–B system

$$\Delta\bar{H}_B = (1-x)^2(-113.4 + 34.5x - 873.9x^2 + 231.0x^3 + 49.6x^4 - 72.5x^5)$$

$$\Delta\bar{S}_B^{ex} = (1-x)^2(-20.9 - 38.0x + 581.7x^2 - 6383.9x^3 + 11850.5x^4 - 26.5x^5)$$

For the Co–B system

$$\Delta\bar{H}_B = (1-x)^2(-117.3 - 222.8x - 809.5x^2 + 2658.4x^3)$$

$$\Delta\bar{S}_B^{ex} = (1-x)^2(-21.8 - 147.4x - 276.5x^2 + 1198.2x^3)$$

For the Ni–B system

$$\Delta\bar{H}_B = (1-x)^2(-127.0 - 116.4x - 3455.9x^2 + 15194.5x^3 - 15050.9x^4)$$

$$\Delta\bar{S}_B^{ex} = (1-x)^2(-18.4 - 31.6x - 410.1x^2 + 1090.5x^3 - 6145.4x^4)$$

The thermodynamic functions of mixing of liquid Fe–B, Co–B and Ni–B alloys calculated with the expressions given above within the concentration ranges of the activity determination are listed in Tables 3, 4 and 5 respectively. The enthalpies and excess Gibbs energies of mixing (the latter at 1900 K) in these systems show large negative values reflecting the strong chemical interaction in the melts. The integral

Table 3
Excess thermodynamic functions of mixing in the Fe–B system at 1900 K[a] ($\Delta H$ and $\Delta G$ in kJ mol$^{-1}$, $\Delta S$ in J mol$^{-1}$ K$^{-1}$)

| $x_B$ | $-\Delta_m\bar{H}_{Fe}$ | $-\Delta_m\bar{H}_B$ | $-\Delta_m H$ | $\Delta_m\bar{S}^{ex}_{Fe}$ | $-\Delta_m\bar{S}^{ex}_B$ | $-\Delta_m S^{ex}$ | $-\Delta_m\bar{G}^{ex}_{Fe}$ | $-\Delta_m\bar{G}^{ex}_B$ | $-\Delta_m G^{ex}$ |
|---|---|---|---|---|---|---|---|---|---|
| 0 | 0 | 113.4±7.3 | 0 | 0 | 20.9±5.2 | 0 | 0 | 73.4±12.0 | 0 |
| 0.04 | 0.2±0.1 | 104.5±7.0 | 4.3±0.4 | 0.0±0.2 | 20.2±4.6 | 0.8±0.3 | 0.1±0.7 | 66.2±11.2 | 2.8±0.7 |
| 0.08 | 0.6±0.4 | 98.3±6.7 | 8.4±0.7 | 0.0±0.3 | 19.5±4.2 | 1.6±0.4 | 0.5±0.9 | 61.3±10.1 | 5.3±1.0 |
| 0.12 | 1.0±0.6 | 94.0±5.4 | 12.2±0.8 | 0.0±0.4 | 19.9±3.4 | 2.4±0.5 | 1.0±1.5 | 56.3±8.4 | 7.6±1.2 |
| 0.16 | 1.5±0.8 | 91.2±5.1 | 15.8±1.0 | 0.3±0.5 | 21.5±3.1 | 3.2±0.6 | 2.0±1.9 | 50.4±7.8 | 9.7±1.5 |
| 0.20 | 1.9±1.1 | 89.3±5.0 | 19.4±1.3 | 0.8±0.7 | 23.9±3.0 | 4.1±0.8 | 3.4±2.5 | 43.9±7.6 | 11.5±1.9 |
| 0.24 | 2.3±1.3 | 87.9±4.6 | 22.8±1.5 | 1.5±0.8 | 26.2±2.8 | 5.2±0.9 | 5.0±3.0 | 38.0±7.0 | 13.0±2.1 |
| 0.28 | 2.8±1.4 | 86.6±4.0 | 26.3±1.5 | 1.9±0.9 | 27.6±2.4 | 6.3±0.9 | 6.4±3.5 | 34.1±6.1 | 14.2±2.2 |
| 0.32 | 3.4±1.4 | 85.1±3.3 | 29.5±1.6 | 1.7±0.9 | 27.0±2.0 | 7.5±0.9 | 6.6±3.5 | 33.7±5.0 | 15.2±2.3 |

[a] Here and in the other tables, confidence bars are given for a confidence limit of 0.95.

Table 4
Excess thermodynamic functions of mixing in the Co–B system at 1900 K ($\Delta H$ and $\Delta G$ in kJ mol$^{-1}$, $\Delta S$ in J mol$^{-1}$ K$^{-1}$)

| $x_B$ | $-\Delta_m\bar{H}_{Co}$ | $-\Delta_m\bar{H}_B$ | $-\Delta_m H$ | $\Delta_m\bar{S}^{ex}_{Co}$ | $-\Delta_m\bar{S}^{ex}_B$ | $-\Delta_m S^{ex}$ | $-\Delta_m\bar{G}^{ex}_{Co}$ | $-\Delta_m\bar{G}^{ex}_B$ | $-\Delta_m G^{ex}$ |
|---|---|---|---|---|---|---|---|---|---|
| 0 | 0 | 117.3±6.0 | 0 | 0 | 21.8±6.0 | 0 | 0 | 75.8±13.5 | 0 |
| 0.04 | 0.0±0.1 | 117.4±5.2 | 4.7±0.3 | 0.1±0.1 | 25.9±5.2 | 1.0±0.2 | 0.2±0.2 | 68.2±12.1 | 2.9±0.5 |
| 0.08 | 0.0±0.3 | 117.6±4.3 | 9.4±0.4 | 0.3±0.2 | 29.4±3.9 | 2.1±0.4 | 0.6±0.4 | 61.2±9.8 | 5.5±0.9 |
| 0.12 | 0.0±0.5 | 117.0±4.1 | 14.1±0.7 | 0.6±0.4 | 32.1±3.2 | 3.3±0.5 | 1.2±0.9 | 56.1±8.1 | 7.8±1.2 |
| 0.16 | 0.4±0.6 | 114.9±4.0 | 18.7±0.8 | 0.8±0.5 | 33.6±3.0 | 4.7±0.6 | 2.0±1.1 | 51.1±7.6 | 9.9±1.4 |
| 0.20 | 1.3±0.9 | 110.7±3.9 | 23.2±1.0 | 0.9±0.6 | 33.7±2.9 | 6.1±0.7 | 3.0±1.5 | 46.5±7.4 | 11.7±1.7 |
| 0.24 | 3.2±1.1 | 104.3±3.6 | 27.4±1.2 | 0.6±0.7 | 32.7±2.7 | 7.4±0.8 | 4.2±1.7 | 42.3±6.9 | 13.3±1.9 |
| 0.28 | 6.2±1.3 | 95.8±3.4 | 31.3±1.3 | −0.3±0.8 | 30.3±2.6 | 8.7±0.9 | 5.6±2.0 | 38.2±6.4 | 14.7±2.1 |
| 0.32 | 10.7±1.4 | 85.3±3.2 | 34.5±1.4 | −1.8±0.9 | 26.8±2.3 | 9.8±1.0 | 7.3±2.2 | 34.8±5.5 | 16.0±2.4 |
| 0.36 | 17.0±1.5 | 73.0±2.8 | 37.2±1.3 | −4.0±1.2 | 22.4±1.9 | 10.7±1.1 | 9.3±2.7 | 34.0±4.7 | 16.9±2.5 |

Table 5
Excess thermodynamic functions of mixing in the Ni–B system at 1900 K ($\Delta H$ and $\Delta G$ in kJ mol$^{-1}$, $\Delta S$ in J mol$^{-1}$ K$^{-1}$)

| $x_B$ | $-\Delta_m\bar{H}_{Ni}$ | $-\Delta_m\bar{H}_B$ | $-\Delta_m H$ | $\Delta_m\bar{S}^{ex}_{Ni}$ | $-\Delta_m\bar{S}^{ex}_B$ | $-\Delta_m S^{ex}$ | $-\Delta_m\bar{G}^{ex}_{Fe}$ | $-\Delta_m\bar{G}^{ex}_B$ | $-\Delta_m G^{ex}$ |
|---|---|---|---|---|---|---|---|---|---|
| 0 | 0 | 127.0±8.2 | 0 | 0 | 18.4±6.5 | 0 | 0 | 91.0±14.8 | 0 |
| 0.04 | 0.1±0.1 | 125.6±7.8 | 5.0±0.4 | 0.1±0.1 | 20.9±6.1 | 0.8±0.3 | 0.1±0.2 | 87.3±13.8 | 3.6±0.7 |
| 0.08 | −0.2±0.1 | 128.0±7.2 | 10.1±0.6 | 0.3±0.2 | 24.7±5.7 | 1.7±0.5 | 0.4±0.4 | 81.9±13.0 | 7.0±1.1 |
| 0.12 | −0.3±0.2 | 130.0±6.6 | 15.3±0.8 | 0.7±0.3 | 28.5±5.3 | 2.8±0.7 | 1.2±0.6 | 75.2±12.0 | 10.1±1.6 |
| 0.16 | −0.1±0.2 | 128.2±6.0 | 20.5±1.0 | 1.2±0.3 | 31.2±4.9 | 4.0±0.8 | 2.4±0.7 | 67.7±11.1 | 12.9±1.8 |
| 0.20 | 1.3±0.3 | 122.2±5.2 | 25.5±1.3 | 1.4±0.4 | 32.2±4.4 | 5.3±0.9 | 4.2±0.8 | 59.8±9.8 | 15.7±2.1 |
| 0.24 | 4.2±0.5 | 112.0±4.9 | 30.1±1.4 | 1.1±0.5 | 31.4±4.0 | 6.7±1.0 | 6.4±1.0 | 51.8±9.0 | 17.2±2.4 |
| 0.28 | 9.0±0.8 | 98.2±4.4 | 34.0±1.5 | 0.2±0.6 | 28.9±3.5 | 7.9±1.1 | 9.1±1.2 | 44.1±8.0 | 19.0±2.6 |
| 0.32 | 15.9±1.1 | 82.3±3.9 | 37.1±1.5 | −1.4±0.7 | 24.9±3.0 | 9.0±1.2 | 12.3±1.4 | 36.8±6.9 | 20.1±2.7 |
| 0.36 | 24.3±1.4 | 65.8±3.5 | 39.3±1.6 | −4.0±0.9 | 19.9±2.8 | 9.8±1.3 | 15.7±1.8 | 30.0±6.4 | 20.9±2.9 |
| 0.40 | 33.9±1.5 | 50.2±2.9 | 40.5±1.6 | −7.4±1.3 | 14.4±2.6 | 10.2±1.4 | 19.5±2.5 | 23.9±5.7 | 21.2±3.1 |
| 0.44 | 43.8±1.6 | 36.7±2.5 | 40.6±1.7 | −11.5±1.6 | 8.8±2.2 | 10.3±1.5 | 23.4±3.1 | 18.5±4.9 | 21.2±3.3 |
| 0.48 | 52.4±1.7 | 26.4±2.0 | 40.0±1.7 | −16.0±2.0 | 3.5±2.0 | 10.0±1.6 | 27.3±3.9 | 13.9±4.3 | 20.8±3.5 |
| 0.50 | 56.1±1.9 | 22.6±1.4 | 39.3±1.8 | −18.3±2.3 | 1.1±1.9 | 9.7±1.9 | 29.2±4.5 | 11.9±3.9 | 20.6±4.0 |

excess entropies of mixing are also characterized by negative values indicating the existence of ordering effects in these liquid alloys. In the Ni–B system, the $\Delta_m S^{ex}$ minimum ($x = 0.43 \pm 0.02$) is located between two congruently melting compounds o-$Ni_4B_3$ and m-$Ni_4B_3$ [21, 22]. In the Fe–B and Co–B systems within the studied concentration ranges, the functions $\Delta_m S^{ex}$ do not reach minimum values. The entropy data for the Fe–B, Co–B and Ni–B systems are close to those reported for Fe–Si, Co–Si and Ni–Si melts. In the silicon systems, the minima are located at 0.51, 0.52 and 0.38 silicon mole fractions, respectively [15]. The minima of $\Delta_m S^{ex}$ in the Fe–B and Co–B systems also correspond to compounds FeB and CoB, respectively [21, 22].

### 3.2. *Thermochemistry of ternary Tr–Fe–B liquid alloys*

Smoothed dependences of the enthalpies of formation and the error bars (confidence limits, 0.95) of the ternary Fe–Cr–B, Fe–Mn–B, Fe–Co–B and Ni–Co–B systems, and of some binary boundary alloys are presented in Tables 6, 7, 8 and 9 respectively. It should be emphasized that the horizontal segments of the partial enthalpies in the Cr–Fe–B and Mn–Fe–B systems in the boron-rich concentration regions correspond to the two-phased fields (liq. + $Cr_5B_3$) and (liq. + $Mn_2B$) or to the formation of ternary borides with similar concentration ratios as the sum of the transition metals to boron. According to the phase diagrams, the intermetallic compound $Cr_5B_3$ fuses incongruently at 2173 K and the $Mn_2B$ compound fuses congruently at 1853 K [21, 22]. The temperatures at which the experiments were carried out in the Cr–Fe–B and Mn–Fe–B systems were about 20 K lower than the fusion temperatures of the mentioned borides. As mentioned above, the thermodynamic functions of the binary boundary Cr–B and Fe–B melts display some micro-inhomogeneity structure. The introduction of a third component in both binary alloys (the ternary Cr–Fe–B system) causes homogenization of the melt, reflected in gradually smoothing dependences of the partial enthalpies of boron. The same effect can be observed in other systems investigated, except in the Ni–B melts. In this case, between 0 and 0.5 mole fractions of nickel increase the microheterogeneous structure of the Ni–Fe–B liquid alloys (the horizontal segments of the boron partial enthalpies in these ternary alloys are wider than in the binary Fe–B melts). The interesting feature of the studied melts is that the partial enthalpies of mixing of Fe, Mn, Co and Ni in the systems Cr–Fe–B, Mn–Fe–B, Co–Fe–B and Ni–Fe–B, respectively, at a 0.25:0.75 concentration ratio of these elements to the other 3d transition metals on the boron-rich side, reach zero or positive values (some of them up to 30 kJ $mol^{-1}$).

The limiting values for infinite dilution of the partial enthalpies of mixing of boron in Tr–Fe alloys versus iron concentration are given in Fig. 2. These functions show positive deviation from the values of the weighted sums. Such behavior indicates that even the weak attractive forces between unlike atoms of the 3d transition metals decrease the pair interaction forces of the metals with boron atoms. One may suggest, as emphasized earlier for the Tr–Fe–C, Tr–Si–B and Tr–Si–C alloys [15], that the well-known simple models of Kohler, Toop, Bonnier, and Muggianu, see Ref. [24], which are usually applicable for the description of ternary melts taking thermodynamic parameters from the corresponding boundary binary melts, would, in most cases, be

Table 6
Partial mixing enthalpies of components in ternary Fe–Cr–B and binary boundary Cr–B melts (in kJ mol$^{-1}$)

| $x_B$ | $(Fe_{0.75}Cr_{0.25})_{1-x}B_x$ | | | $(Fe_{0.50}Cr_{0.50})_{1-x}B_x$ | | | $(Fe_{0.25}Cr_{0.75})_{1-x}B_x$ | | | $Cr_{1-x}B_x$ | |
|---|---|---|---|---|---|---|---|---|---|---|---|
| | $-\Delta\bar{H}_{Fe}$ | $\Delta\bar{H}_{Cr}$ | $-\Delta\bar{H}_B$ | $-\Delta\bar{H}_{Fe}$ | $\Delta\bar{H}_{Cr}$ | $-\Delta\bar{H}_B$ | $\Delta\bar{H}_{Fe}$ | $-\Delta\bar{H}_{Cr}$ | $-\Delta H_B$ | $-\Delta\bar{H}_{Cr}$ | $-\Delta\bar{H}_B$ |
| 0 | 0.4±0.3 | −9.7±1.9 | 113.8±7.3 | 3.7±1.1 | −4.5±1.2 | 113.6±6.9 | −10.0±1.8 | 0.7±0.4 | 120.5±6.3 | 0 | 141.6±5.4 |
| 0.04 | 0.9±0.4 | −8.8±1.7 | 107.1±7.0 | 5.2±0.9 | −2.5±1.0 | 114.4±6.4 | −1.8±1.4 | 3.3±0.5 | 126.2±5.8 | 0.1±0.1 | 141.3±5.1 |
| 0.08 | 2.6±0.6 | −6.0±1.6 | 98.5±6.8 | 7.9±0.8 | −0.3±0.9 | 108.6±6.1 | 3.5±1.2 | 5.7±0.6 | 120.5±5.6 | 0.9±0.2 | 129.1±4.8 |
| 0.12 | 5.0±0.8 | −2.0±1.5 | 91.5±6.6 | 11.0±1.0 | 1.8±0.9 | 103.0±5.9 | 7.1±1.4 | 7.9±0.8 | 113.8±5.3 | 2.1±0.2 | 117.9±4.6 |
| 0.16 | 7.6±1.1 | 3.0±1.5 | 88.6±6.5 | 14.0±1.2 | 4.0±0.9 | 100.6±5.8 | 9.8±1.6 | 9.1±1.0 | 110.7±5.0 | 2.8±0.3 | 113.3±4.4 |
| 0.20 | 10.0±1.5 | 7.6±1.6 | 84.9±6.5 | 16.3±1.5 | 5.6±1.0 | 98.9±5.7 | 12.1±1.9 | 10.3±1.3 | 107.9±4.9 | 3.5±0.4 | 110.4±4.3 |
| 0.24 | 12.0±1.8 | 8.9±1.8 | 80.7±6.5 | 17.8±1.8 | 4.0±1.1 | 93.1±5.8 | 14.6±2.2 | 13.6±1.7 | 99.2±4.9 | 6.3±0.6 | 100.7±4.1 |
| 0.28 | 14.0±2.2 | 5.2±2.0 | 74.4±6.7 | 18.5±2.1 | −2.0±1.3 | 83.0±6.0 | 17.2±2.5 | 20.3±2.1 | 84.7±5.2 | 12.0±0.8 | 84.3±4.2 |
| 0.32 | 16.4±2.6 | 4.0±2.2 | 69.7±7.0 | 18.5±2.5 | −2.0±1.5 | 83.0±6.2 | 20.8±2.8 | 22.6±2.6 | 79.4±5.4 | 13.1±1.4 | 81.2±4.6 |

Table 7
Partial mixing enthalpies of components in ternary Fe–Mn–B and binary boundary Mn–B melts (in kJ mol$^{-1}$)

| $x_B$ | $(Fe_{0.75}Mn_{0.25})_{1-x}B_x$ | | | $(Fe_{0.50}Mn_{0.50})_{1-x}B_x$ | | | $(Fe_{0.25}Mn_{0.75})_{1-x}B_x$ | | | $Mn_{1-x}B_x$ | |
|---|---|---|---|---|---|---|---|---|---|---|---|
| | $-\Delta\bar{H}_{Fe}$ | $-\Delta\bar{H}_{Mn}$ | $-\Delta\bar{H}_B$ | $-\Delta\bar{H}_{Fe}$ | $-\Delta\bar{H}_{Mn}$ | $-\Delta\bar{H}_B$ | $-\Delta\bar{H}_{Fe}$ | $-\Delta\bar{H}_{Mn}$ | $-\Delta H_B$ | $-\Delta\bar{H}_{Mn}$ | $-\Delta\bar{H}_B$ |
| 0 | 0.3±0.2 | 11.1±1.6 | 98.2±11.3 | 3.1±2.3 | 6.7±1.3 | 89.4±9.1 | 11.1±2.5 | 2.1±0.5 | 95.2±6.4 | 0 | 112.1±5.3 |
| 0.04 | 1.2±0.3 | 9.7±1.3 | 93.4±9.7 | 4.9±1.8 | 5.2±1.1 | 87.8±7.3 | 12.0±2.1 | 1.6±0.4 | 92.7±6.1 | 0.1±0.1 | 109.4±5.0 |
| 0.08 | 2.3±0.4 | 8.9±1.1 | 89.2±8.5 | 6.4±1.5 | 4.3±1.0 | 84.6±6.7 | 12.2±1.8 | 1.4±0.4 | 92.1±5.9 | 0.2±0.1 | 107.5±4.8 |
| 0.12 | 3.3±0.5 | 8.1±1.0 | 83.6±7.7 | 7.4±1.4 | 3.7±0.9 | 82.4±6.2 | 11.6±1.6 | 1.5±0.5 | 92.3±5.7 | 0.4±0.2 | 105.2±4.6 |
| 0.16 | 4.2±0.6 | 7.1±0.9 | 80.6±7.3 | 8.1±1.4 | 3.3±0.8 | 81.8±6.0 | 10.6±1.6 | 1.8±0.5 | 92.5±5.5 | 1.0±0.5 | 101.8±4.6 |
| 0.20 | 4.9±0.7 | 5.8±0.9 | 79.2±7.0 | 8.4±1.5 | 3.1±0.8 | 81.0±6.0 | 9.1±1.6 | 2.5±0.6 | 91.9±5.4 | 2.1±0.7 | 96.8±4.8 |
| 0.24 | 5.6±0.8 | 4.4±0.8 | 78.5±6.8 | 8.6±1.6 | 3.1±0.8 | 80.1±5.9 | 7.7±1.7 | 3.8±0.7 | 89.9±5.4 | 4.1±0.9 | 89.8±5.1 |
| 0.28 | 6.8±1.0 | 2.8±0.7 | 77.1±6.8 | 8.7±1.7 | 3.6±0.9 | 76.6±5.8 | 6.7±1.8 | 5.8±0.7 | 86.0±5.6 | 7.3±1.1 | 80.8±5.5 |
| 0.32 | 9.1±1.2 | 1.5±0.8 | 74.0±6.9 | 8.7±1.9 | 3.6±1.0 | 76.6±5.9 | 7.2±1.9 | 8.9±0.8 | 79.9±5.8 | 7.9±1.3 | 78.2±5.8 |
| 0.36 | 13.4±1.5 | 0.4±0.9 | 68.2±7.0 | 8.7±2.2 | 3.6±1.1 | 76.6±6.2 | 10.1±2.0 | 13.2±1.0 | 71.5±6.0 | 7.9±1.4 | 78.2±6.2 |
| 0.40 | 13.4±1.6 | 0.4±1.2 | 68.2±7.3 | 8.7±2.6 | 3.6±1.3 | 76.6±6.5 | 10.1±2.3 | 13.2±1.3 | 71.5±6.2 | 7.9±1.7 | 78.2±6.8 |

Table 8
Partial mixing enthalpies of components in ternary Fe–Co–B melts (in kJ mol$^{-1}$)

| $x_B$ | $(Fe_{0.75}Co_{0.25})_{1-x}B_x$ | | | $(Fe_{0.50}Co_{0.50})_{1-x}B_x$ | | | $(Fe_{0.25}Co_{0.75})_{1-x}B_x$ | | |
|---|---|---|---|---|---|---|---|---|---|
| | $-\Delta\bar{H}_{Fe}$ | $\Delta\bar{H}_{Co}$ | $-\Delta\bar{H}_B$ | $-\Delta\bar{H}_{Fe}$ | $\Delta\bar{H}_{Co}$ | $-\Delta\bar{H}_B$ | $-\Delta\bar{H}_{Fe}$ | $\Delta\bar{H}_{Co}$ | $-\Delta H_B$ |
| 0 | 0.3±0.3 | −5.7±1.5 | 100.6±7.4 | 2.2±0.6 | −2.7±0.7 | 95.6±6.7 | 5.7±1.3 | −0.6±0.4 | 99.9±6.4 |
| 0.04 | 2.4±0.3 | 0.3±1.3 | 98.7±6.8 | 3.8±0.7 | −0.7±0.6 | 93.8±6.3 | 4.6±1.1 | −0.6±0.3 | 97.2±6.1 |
| 0.08 | 4.7±0.4 | 6.4±1.5 | 94.8±6.3 | 6.1±0.9 | 1.6±0.6 | 91.7±5.9 | 4.8±0.9 | −0.2±0.3 | 96.7±5.8 |
| 0.12 | 7.1±0.6 | 12.5±1.8 | 91.4±5.8 | 8.6±1.1 | 4.3±0.7 | 90.1±5.6 | 5.8±0.9 | 0.3±0.5 | 96.4±5.6 |
| 0.16 | 9.3±0.7 | 18.1±2.1 | 89.2±5.5 | 11.3±1.2 | 6.8±0.8 | 88.5±5.3 | 7.6±1.1 | 0.8±0.7 | 95.2±5.3 |
| 0.20 | 11.2±0.9 | 23.0±2.5 | 87.3±5.2 | 13.9±1.3 | 8.9±1.0 | 86.6±5.0 | 9.2±1.3 | 0.9±0.9 | 92.6±5.1 |
| 0.24 | 13.2±1.1 | 26.7±2.8 | 85.1±4.7 | 16.7±1.4 | 10.2±1.2 | 83.6±4.7 | 12.8±1.5 | 0.4±1.1 | 88.5±4.9 |
| 0.28 | 15.4±1.3 | 29.2±3.2 | 82.7±4.3 | 19.8±1.5 | 10.4±1.3 | 79.3±4.4 | 16.4±1.8 | −1.2±1.3 | 82.7±4.7 |
| 0.32 | 18.6±1.5 | 30.0±3.6 | 76.4±3.8 | 24.1±1.8 | 9.2±1.5 | 73.1±4.1 | 21.5±2.1 | −4.0±1.5 | 75.2±4.7 |
| 0.36 | 23.7±1.8 | 28.9±4.1 | 68.5±3.9 | 30.4±2.1 | 6.7±1.7 | 64.8±4.2 | 28.8±2.5 | −8.1±1.7 | 66.2±4.9 |
| 0.40 | 32.0±2.2 | 26.2±4.6 | 57.3±4.2 | 39.8±2.5 | 2.7±2.0 | 54.4±4.5 | 39.6±3.0 | −13.4±2.0 | 55.9±5.3 |

Table 9
Partial mixing enthalpies of components in ternary Fe–Ni–B melts (in kJ mol$^{-1}$)

| $x_B$ | $(Fe_{0.75}Ni_{0.25})_{1-x}B_x$ | | | $(Fe_{0.50}Ni_{0.50})_{1-x}B_x$ | | | $(Fe_{0.25}Ni_{0.75})_{1-x}B_x$ | | | $(Fe_{0.10}Ni_{0.90})_{1-x}B_x$ | | |
|---|---|---|---|---|---|---|---|---|---|---|---|---|
| | $-\Delta\bar{H}_{Fe}$ | $\Delta\bar{H}_{Ni}$ | $-\Delta\bar{H}_B$ | $-\Delta\bar{H}_{Fe}$ | $-\Delta\bar{H}_{Ni}$ | $-\Delta\bar{H}_B$ | $-\Delta\bar{H}_{Fe}$ | $-\Delta\bar{H}_{Ni}$ | $-\Delta H_B$ | $-\Delta\bar{H}_{Fe}$ | $-\Delta\bar{H}_{Ni}$ | $-\Delta\bar{H}_B$ |
| 0 | 0.2±0.2 | −8.5±1.6 | 104.3±7.7 | 1.3±0.4 | 7.0±1.1 | 100.0±7.0 | 8.6±1.5 | 3.0±0.7 | 97.9±6.4 | 20.3±2.1 | 0.6±0.5 | 116.9±8.0 |
| 0.04 | 2.7±0.4 | −1.3±1.2 | 97.6±7.3 | 2.6±0.6 | 7.3±0.9 | 97.4±6.5 | 7.7±1.3 | 3.6±0.5 | 99.6±6.1 | 18.8±1.8 | 0.5±0.4 | 113.3±7.4 |
| 0.08 | 5.2±0.7 | 4.5±1.4 | 88.4±7.0 | 4.7±0.8 | 7.1±0.8 | 94.3±6.1 | 8.6±1.2 | 3.6±0.5 | 99.2±5.7 | 19.7±1.6 | 0.2±0.3 | 110.0±6.9 |
| 0.12 | 7.4±0.9 | 8.7±1.9 | 82.4±6.7 | 6.8±0.9 | 6.7±1.0 | 87.1±5.8 | 10.2±1.2 | 3.4±0.5 | 98.7±5.5 | 20.7±1.5 | 0.0±0.5 | 107.3±6.4 |
| 0.16 | 9.2±1.3 | 11.5±2.1 | 78.9±6.4 | 8.7±1.1 | 6.3±1.2 | 82.0±5.5 | 12.1±1.3 | 3.3±0.6 | 96.0±5.3 | 22.7±1.7 | 0.1±0.7 | 104.4±6.0 |
| 0.20 | 10.3±1.8 | 12.7±2.3 | 77.0±6.2 | 10.2±1.3 | 6.3±1.4 | 78.3±5.1 | 13.6±1.5 | 3.8±0.8 | 91.4±5.1 | 24.3±1.9 | 1.0±1.1 | 99.5±5.7 |
| 0.24 | 10.9±2.3 | 12.2±2.4 | 75.8±6.0 | 11.0±1.5 | 7.1±1.7 | 75.1±5.5 | 14.7±1.9 | 5.2±1.1 | 85.0±5.0 | 25.4±2.2 | 3.0±1.6 | 92.3±5.5 |
| 0.28 | 11.4±2.8 | 10.1±2.5 | 74.0±5.9 | 11.5±1.7 | 8.9±1.9 | 71.4±5.9 | 15.3±2.3 | 7.8±1.4 | 76.8±5.0 | 25.9±2.4 | 6.4±2.0 | 84.4±5.4 |
| 0.32 | 12.5±3.5 | 6.2±2.5 | 70.6±5.9 | 12.3±2.0 | 12.1±2.1 | 66.6±6.4 | 16.0±2.7 | 11.9±1.6 | 66.7±5.2 | 26.2±2.7 | 11.5±2.6 | 74.3±5.5 |
| 0.36 | 15.1±4.1 | 0.4±2.6 | 64.7±6.1 | 14.4±2.4 | 16.9±2.3 | 59.9±7.0 | 17.6±3.3 | 17.7±2.0 | 54.9±5.5 | 27.2±3.3 | 18.4±3.3 | 62.8±5.9 |
| 0.40 | 20.4±4.7 | −7.1±2.8 | 55.5±6.5 | 18.8±2.9 | 23.4±2.6 | 50.9±8.7 | 21.2±3.9 | 25.3±2.7 | 41.6±6.0 | 30.0±3.7 | 27.1±3.7 | 50.1±6.5 |

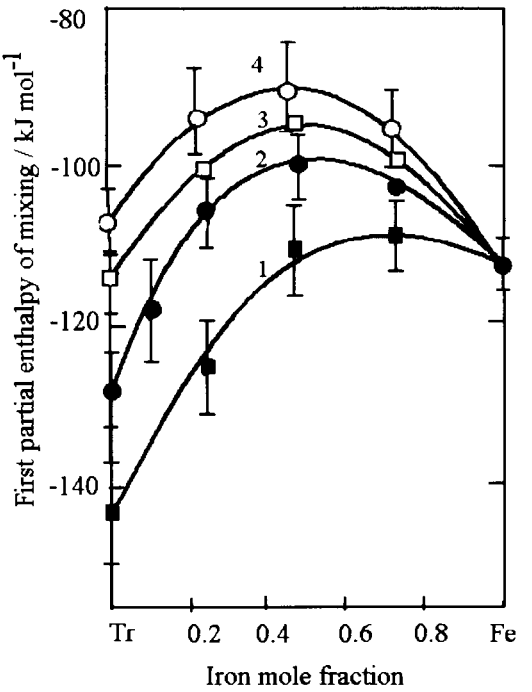


Fig. 2. Limiting partial mixing enthalpies of boron vs. iron concentration in ultimately dilute alloys: curve 1, Cr–Fe; curve 2, Ni–Fe; curve 3, Co–Fe; curve 4, Mn–Fe.

incorrect for Tr–Fe–B systems. This conclusion was actually confirmed by comparison of the data calculated using these formulae with the experimental data for the melts on ray sections $x_{Tr}:x_{Fe} = 0.5:0.5$ (Fig. 1).

The isolines of the integral enthalpies of mixing referred to liquid 3d transition metals and undercooled liquid boron are given in Fig. 3. As can be seen, all the investigated systems possess significant negative values of these integral enthalpies of formation. This fact confirms that strong attractive interactions between unlike particles actually exist in such melts and is consistent with the presence of several binary and ternary intermetallic compounds in the respective Tr–Fe–B systems.

### *3.3. Glass-forming ability of the Tr–Fe–B melts*

It is of current interest to estimate the glass forming tendency (GFT) of the investigated systems. Earlier, Zielinski and Matija's approach, modified for ternary alloys, was successfully applied for ternary alloys characterized by high energies of interaction of two metalloid components with a 3d transition metal [15]. The principal equation is expressed as follows (in a previous publication, the exponent $(m + n + l)$ in

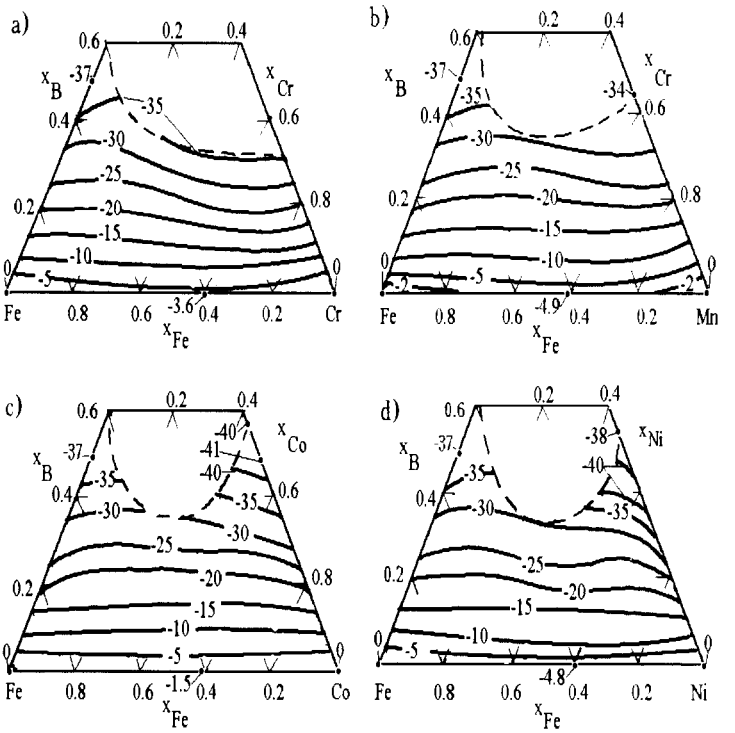


Fig. 3. Integral enthalpies of formation of ternary alloys in Tr–Fe–B systems, the reference state being liquid metals and liquid boron (kJ $mol^{-1}$): (a) Cr–Fe–B system at 2150 K; (b) Mn–Fe–B system at 1830 K; (c) Co–Fe–B system at 1900 K; (d) Ni–Fe–B system at 1873 K.

this formula was incorrectly given as a multiplier)

$$\mathrm{GFT} = -\log\left[1-\frac{2\Delta_m H(x,y)}{(x_a+y_a)RT}\right] - 0.434\left[\frac{\Delta_m H(x,y)}{(x_a+y_a)RT}+\left(\frac{x+y}{x_a+y_a}\right)^{(m+n+l)}\log\left(\frac{N}{m+n+l}\right)\right]$$

where $\Delta_m H(x,y)$ is the integral enthalpy of mixing in ternary liquid alloys versus the second ($x$) and third ($y$) component mole fractions; $x_a$ and $y_a$ denote the concentrations corresponding to the formation of structural groups promoting the nucleation act ($x_a = n/(m+n+l)$ and $y_a = l/(m+n+l)$ $m$, $n$ and $l$ are the stoichiometric coefficients of the structural group (cluster) corresponding to the first, second and third components respectively; $R$ is the gas constant; $T$ is the temperature to which similar melts can be supercooled; and $N$ is Avogadro's number.

In these ternary systems, the pair interactions between iron and other transition metals are weak and, according to the phase diagrams [25], mixed borides $(Fe,Tr)_3B$, $(Fe, Tr)_2B$ and (Fe, Tr)B are formed. For this reason, in such cases it is more logical to

Table 10
Cluster types defined from the partial enthalpy functions

| System | Cluster type for ray section with constant ratio $x_{Tr}:x_{Fe}$ | | | | |
|---|---|---|---|---|---|
| | 0.10 | 0.25:0.75 | 0.5:0.5 | 0.75:0.25 | 1.0:0 |
| Fe–Cr–B | $Fe_2B$ | $(Fe,Cr)_2B$ | $(Fe,Cr)_2B$ | $(Fe,Cr)_3B$ | $Cr_3B$ |
| Fe–Mn–B | $Fe_2B$ | $(Fe,Mn)_2B$ | $(Fe,Mn)_3B$ | $(Fe,Mn)_2B$ | $Mn_2B$ |
| Fe–Co–B | $Fe_2B$ | $(Fe,Co)_3B$ | $(Fe,Co)_3B$ | $(Fe,Co)_3B$ | $Co_2B$ |
| Fe–Ni–B | $Fe_2B$ | $(Fe,Ni)_3B$ | $(Fe,Ni)_3B$ | $(Fe,Ni)_3B$ | $Ni_3B$ |

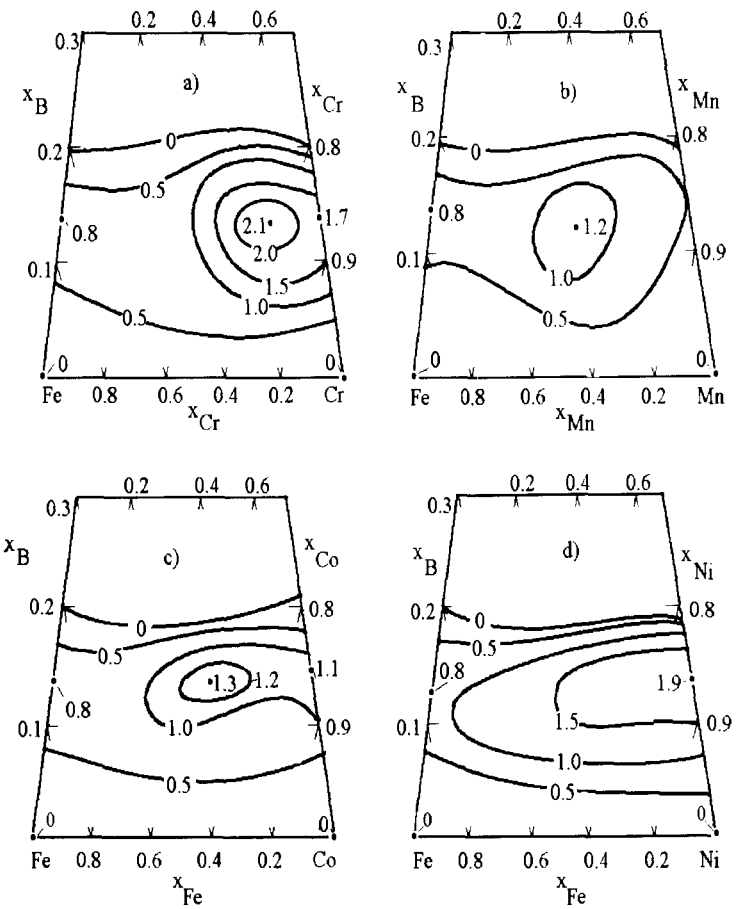


Fig. 4. Glass-forming ability of Tr–Fe–B melts: (a) Cr–Fe–B system; (b) Mn–Fe–B system; (c) Co–Fe–B system; (d) Ni–Fe–B system.

assess the glass-forming tendency using the following simplified equation

$$\mathrm{GFT} = -\log\left[1-\frac{2(m+n)\Delta_m H(x)}{nRT}\right] - 0.434\left[\frac{(m+n)\Delta_m H(x)}{nRT}+\left(x\frac{m+n}{n}\right)^{(m+n)}\log\left(\frac{N}{m+n}\right)\right]$$

where $\Delta_m H(x)$ is the integral enthalpy of mixing in liquid alloys with a constant ratio of $x_{Fe}/x_{Tr}$: boron mole fraction $x$. Stoichiometric indexes of clusters were determined using the same principle as described in Ref. [15] and $T$ was taken to be 1000 K. Clusters considered as nuclei of crystallization are listed in Table 10. Calculated GFT surfaces (positive isolines are given in Fig. 4) around the compositions $Mn_{0.47}Fe_{0.40}B_{0.13}$, $Co_{0.56}Fe_{0.30}B_{0.14}$, $Ni_{0.87}B_{0.13}$ and $Cr_{0.70}Fe_{0.17}B_{0.13}$, show maxima which reveal the most favorable compositions for the formation of amorphous alloys. Values of the maxima indicate increasing the glass-forming ability in accordance with the sequence of compositions given above.

## Acknowledgements

The author is grateful to Dr. M. Ivanov for helpful discussions and comments on the manuscript. This work was supported by the International Science Foundation and by the Fundamental Investigations State Foundation of the Ukraine.

## References

[1] M. Yukinobu, O. Ogawa and S. Goto, Metall. Trans. B, 20 (1989) 705.
[2] R. Ushio and O. Ogawa, Metall. Trans. B, 22 (1991) 47.
[3] E.K. Storms and E.G. Szklarz, J. Less-Common Met., 135 (1987) 229.
[4] V.T. Witusiewicz, A.A. Stsheretski and V.S. Shumikhin, Rasplavy, 4 (1989) 102.
[5] V.T. Witusiewicz, A.A. Stsheretski and V.S. Shumikhin, Rasplavy, 1 (1990) 82.
[6] V.T. Witusiewicz, A.A. Stsheretski and A.K. Biletski, Metally (Rep. Sov. Acad. Sci.), 4 (1990) 199.
[7] V.T. Witusiewicz, A.A. Stsheretski and V.S. Shumikhin, Metally (Rep. Sov. Acad. Sci.), 5 (1990) 52.
[8] V.T. Witusiewicz and V.S. Shumikhin, Rasplavy, 4 (1992) 85.
[9] V.T. Witusiewicz, Metally (Rep. Russ. Acad. Sci.), 3 (1993) 35.
[10] V.T. Witusiewicz, Metally (Rep. Russ. Acad. Sci.), 4 (1993) 38.
[11] V.T. Witusiewicz, A.A. Stsheretski and V.S. Shumikhin, Rasplavy, 6 (1988) 72.
[12] J.F. Elliott, M. Gleiser and V. Ramakrishna, Thermochemistry for Steelmaking, Metallurgiya Publ., Moscow, 1969 (in Russian).
[13] V.P. Glushko (Ed.), Thermodynamic Properties of Individual Substances, Nauka, Moscow, 1978–1982.
[14] V.T. Witusiewicz and M.I. Ivanov, J. Alloys Comp., 200 (1993) 177.
[15] V.T. Witusiewicz, J. Alloys Comp., 203 (1994) 103.
[16] V.T. Witusiewicz, A.K. Biletski and V.S. Shumikhin, Metally (Rep. Sov. Acad. Sci.), 3 (1987) 62.
[17] P. Roy and R. Hultgren, Trans. Met. Soc. AIME, 233 (1965) 1811.
[18] Y. Iguchi and Y. Tozaki, J. Iron Steel Inst. Jpn., 67 (1981) 925.
[19] Y. Iguchi, S. Nobory, K.Saito and T. Fuwa, J. Iron Steel Inst. Jpn., 68 (1982) 633.
[20] N.B. Ageev (Ed.), Phase Diagrams of the Metallic Systems, Published 1970, VINITI, Moscow, 1972.

[21] T.B. Massalski (Ed.), Binary Alloy Phase Diagrams, ASM, Materials Park, OH, 1990.
[22] H. Baker (Ed.), ASM Handbook, Vol. 3. Alloy Phase Diagram, ASM, Materials Park, OH, 1992.
[23] P.G. Zielinski and H. Matyja, in N.J. Grant (Ed.), Rapidly Quenched Metals, MIT Press, Cambridge MA, 1975, pp. 237–248.
[24] R. Lück, U. Gerling and B. Predel, Z. Metallk., 77 (1986) 442.
[25] G. Pradelli, C. Gianoglio and E. Quadrini, Metall. Ital., 7/8 (1981) 351.